

RESEARCH ARTICLE | NOVEMBER 22 2022

## Challenges and opportunities in free-standing supercapacitors research <sup>EP</sup>

Special Collection: [Materials Challenges for Supercapacitors](#)

Kenneth G. Latham <sup>ORCID</sup>; Anjali Achazhiyath Edathil <sup>ORCID</sup>; Babak Rezaei; Sihui Liu; Sang Nguyen; Stephan Sylvest Keller <sup>ORCID</sup>; Felice Torrisci <sup>ORCID</sup>; Emile S. Greenhalgh; Maria-Magdalena Titirici <sup>ORCID</sup> ✉

Check for updates

APL Mater. 10, 110903 (2022)  
<https://doi.org/10.1063/5.0123453>

View Online

Export Citation

CrossMark

**AMERICAN ELEMENTS**  
 THE ADVANCED MATERIALS MANUFACTURER®

yttrium-iron garnet, glassy carbon, benzophenone, fused quartz, additive manufacturing  
 azobites, Si-Ni semiconductors, gallium lens, copper nanoparticles, organometallics  
 seleno diborates, barium fluoride, tungsten phosphor, photonics, wettable dyes  
 sapphire windows, NiTiVAG, epitaxial crystal growth, ultra-high purity materials, transparent ceramics, CVD  
 spherulites, seleno substrates, ceramic-grade polishing powder, B, C, N, O, F, Ne  
 silver nanoparticles, perovskites, surface-functionalized nanoparticles, Al, Si, P, S, Cl, Ar  
 MOCVD, beta-barium borate, surface-functionalized nanoparticles, Al, Si, P, S, Cl, Ar  
 rare earth metals, quantum dots, surface-functionalized nanoparticles, Al, Si, P, S, Cl, Ar  
 emulsion, acidification Ca-VAG, surface-functionalized nanoparticles, Al, Si, P, S, Cl, Ar  
 refractory metals, laser crystals, surface-functionalized nanoparticles, Al, Si, P, S, Cl, Ar  
 nitride semiconductors, SiAs wafers, surface-functionalized nanoparticles, Al, Si, P, S, Cl, Ar  
 MOFs, AuNPs, surface-functionalized nanoparticles, Al, Si, P, S, Cl, Ar  
 2D, C60, surface-functionalized nanoparticles, Al, Si, P, S, Cl, Ar  
 nonstoichiometric crystals, inorganic ceramics, surface-functionalized nanoparticles, Al, Si, P, S, Cl, Ar

silicon nitride, MgO, water, diamond micropowders, optical glass

**Now Invent.™**

[www.americanelements.com](http://www.americanelements.com)

© 2021-22 American Elements LLC. All Rights Reserved. Drexel 44

# Challenges and opportunities in free-standing supercapacitors research

Cite as: APL Mater. 10, 110903 (2022); doi: 10.1063/5.0123453

Submitted: 30 August 2022 • Accepted: 3 November 2022 •

Published Online: 22 November 2022



View Online



Export Citation



CrossMark

Kenneth G. Latham,<sup>1</sup>  Anjali Achazhiyath Edathil,<sup>2</sup>  Babak Rezaei,<sup>2</sup> Sihui Liu,<sup>3</sup> Sang Nguyen,<sup>4</sup> Stephan Sylvest Keller,<sup>2</sup>  Felice Torrisi,<sup>3,5,6</sup>  Emile S. Greenhalgh,<sup>4</sup> and Maria-Magdalena Titirici<sup>1,a)</sup> 

## AFFILIATIONS

<sup>1</sup>Department of Chemical Engineering, Imperial College London, South Kensington Campus, London SW7 2AZ, United Kingdom

<sup>2</sup>National Centre for Nano Fabrication and Characterization, DTU Nanolab, Technical University of Denmark, 2800 Kgs. Lyngby, Denmark

<sup>3</sup>Molecular Sciences Research Hub, Department of Chemistry, Imperial College London, White City Campus, 82 Wood Lane, London W12 0BZ, United Kingdom

<sup>4</sup>Department of Aeronautics, Imperial College London, South Kensington Campus, London SW7 2AZ, United Kingdom

<sup>5</sup>Dipartimento di Fisica e Astronomia, Universita' di Catania, Via S. Sofia 64, 95123 Catania, Italy

<sup>6</sup>CNR-IMM (Catania Università), Via S. Sofia 64, Catania 95123, Italy

**Note:** This paper is part of the Special Topic on Materials Challenges for Supercapacitors.

<sup>a)</sup>Author to whom correspondence should be addressed: [m.titirici@imperial.ac.uk](mailto:m.titirici@imperial.ac.uk)

## ABSTRACT

The design of commercial supercapacitors has remained largely unchanged since the 1970s, comprising powdered electrodes housed in rigid metal cylinders or pouches. To power the next generation of integrated technologies, an evolution in supercapacitor materials and design is needed to create multifunctional materials that allow energy storage while imparting additional material properties (e.g., flexibility and strength). Conductive free-standing electrodes produced from fibers or 3D printed materials offer this opportunity as their intrinsic mechanical properties can be transferred to the supercapacitor. Additionally, their conductive nature allows for the removal of binders, conductive agents, and current collectors from the supercapacitor devices, lowering their economic and environmental cost. In this Perspective, we summarize the recent progress on free-standing supercapacitors from new methods to create free-standing electrodes to novel applications for these devices, together with a detailed discussion and analysis on their electrochemical performance and physicochemical and mechanical properties. Furthermore, the potential directions and prospects of future research in developing free-standing supercapacitors are proposed.

© 2022 Author(s). All article content, except where otherwise noted, is licensed under a Creative Commons Attribution (CC BY) license (<http://creativecommons.org/licenses/by/4.0/>). <https://doi.org/10.1063/5.0123453>

## I. INTRODUCTION

Supercapacitors, also known as electrochemical capacitors, have received considerable attention over the past several decades due to their superior power density ( $10^2$ – $10^5$  W kg<sup>-1</sup>), fast charge–discharge rates (s to mins), Coulombic efficiency (>98%), and high cycle life (>500 000).<sup>1</sup> As a result, they are presently deployed in a wide range of commercial applications, such as renewable energy load leveling, consumer electronics, computer memory

backup, regenerative braking, and electric vehicles.<sup>2–6</sup> Currently, there are three main types of supercapacitors, electrical double layer capacitors (EDLCs), pseudocapacitors, and hybrid capacitors. These types all follow the same basic architecture with a positive electrode and a negative electrode kept apart by an electrolyte-soaked separator material. The difference between them is the method of electrochemical energy storage. EDLCs store energy through electrostatic charge accumulation/release at the electrode/electrolyte interface using high surface area electrodes.<sup>7</sup> Pseudocapacitors store energy at

the electrode surface through highly reversible oxidation/reduction (redox) or Faradaic reactions of electro-active electrode materials.<sup>8</sup> Alternatively, hybrid capacitors combine a supercapacitor electrode [e.g., activated carbon (AC)] with a battery style anode (e.g., graphite).<sup>9</sup> Important benchmark values for supercapacitors are their energy density (charge stored per unit volume) and power density (charge rate delivered per unit volume). Energy density for a supercapacitor is proportional to its capacity ( $C$ ) and the square of the potential window ( $V$ ). Power density is the square of the potential window ( $V$ ) divided by four times the equivalent series resistance ( $R_s$ ). Supercapacitors inherently have a high-power density, so the focus of the main body of supercapacitor research has revolved around enhancing energy density. This can be achieved in two ways: increasing the capacitance or expanding the voltage window. For EDLCs, capacitance can be improved by increasing the available electroactive surface area through porosity development, whereas capacitance in pseudocapacitors is enhanced by increasing the number of electroactive groups. The voltage window is governed by the electrical decomposition point of the electrolyte, so improvements can be gained by using electrolytes with expanded voltage windows (e.g., ionic liquids). Further information on the fundamentals of supercapacitors, types, and electrolytes can be found in the several recent publications.<sup>8–13</sup>

Commercial supercapacitors are predominately carbon-based EDLCs constructed using two symmetrical porous carbon electrodes each bound to a current collector. These electrodes are kept apart by an organic electrolyte-soaked separator material. To form the carbon electrodes, the powdered electroactive material is mixed with binders, conductive agents, and solvents to form a slurry that is coated onto a current collector foil. The binder, typically a fluorine containing insulating polymer, such as poly(vinylidene-difluoride) (PVdF), is needed to form a solid electrode, while the conductive agent (e.g., carbon black and graphite) improves the charge transfer. Unfortunately, these components contribute negligible amounts of charge storage; give rise to resistive interfaces between the active material, binder, and current collector; and occupy space and weight in the supercapacitor, lowering the overall volumetric and gravimetric energy density.<sup>14</sup> Additionally, there are environmental and economic concerns around the use of fluorinated binders and the teratogen and toxic N-methyl-2-pyrindone (NMP) solvent commonly used in electrode casting.<sup>15</sup> Finally, to form the supercapacitor device, the electrodes are wound or folded into a cylindrical or rectangular shape to be installed inside a rigid cylinder or rectangular housing, preventing flexibility and limiting the applications and locations where supercapacitors can be installed.

Substituting powdered carbon electrodes with a conductive free-standing electrode allows for the omission of current collectors, insulating binders, conductive agents, and solvents as free-standing electrodes play the role of current collector and active material. Removing the current collector can lower the weight of the supercapacitor by 20%–30% and lower the cost of the electrode by 59%.<sup>7</sup> Free-standing electrodes can also be designed to provide unique mechanical properties to the supercapacitor, unlocking new technologies. For instance, flexible fiber electrodes can be interwoven into textiles to improve strength while providing energy storage, while three-dimensional (3D) printed electrodes can be moulded around device components. In this Perspective, we will discuss the latest advancements, challenges, and outlook for

free-standing supercapacitors. It will be structured into two parts: the first examining advancements in supercapacitor components using carbon fibers, 3D printed electrodes, and new electrolyte developments, while Sec. II will discuss unique applications for free-standing electrodes.

## II. FREE-STANDING SUPERCAPACITOR COMPONENTS

### A. Free-standing carbon fiber mat electrodes

Free-standing carbon fibers in single, entangled, or interwoven configurations hold an enormous potential as electrodes in energy storage applications. Carbon fibers are lightweight, easy to handle, flexible, highly conductive, and chemically stable in a wide range of electrolytes (i.e., acidic, alkaline, organic, and ionic liquid). These materials also naturally exhibit double layer capacitance, allowing them to be utilized as EDLC electrodes in flexible, wearable, and mouldable energy storage applications.<sup>14,16,17</sup>

Several spinning techniques can be used to create carbon fibers suitable for EDLCs and pseudocapacitors. Melt, wet, and dry spinning techniques produce single micrometer diameter sized polymer fibers with high tensile strength that can be wound onto a spool.<sup>18</sup> These are applicable in creating single-, coaxial-, or multi-fiber supercapacitors that can be interwoven into textiles, integrated into wires, and form sensor networks. Alternatively, electrospinning and centrifugal spinning can easily create large flexible non-woven 3D mats of submicrometer diameter polymer fibers suitable for larger free-standing flexible electrodes.<sup>14,19</sup> To create carbon fibers from these techniques, the spun polymer fiber is typically stabilized in air at low temperature (<300 °C) before being carbonized at high temperature (>800 °C) to form the carbon fiber. In-depth information on each of these techniques can be found in Refs. 14, 18, 20, and 21.

Despite the advancements in electrospinning over the last decade, the performance of electrospun carbon fiber mats (CFMs) is still lower than powder-based electrodes. Initially, similar methods used for enhancing powdered electrodes were applied to carbon CFMs (e.g., templates<sup>22–25</sup> and activation agents<sup>26,27</sup>). This worked by increasing the surface area, which in turn enhanced the capacitance and improved the energy density of the carbon fibers.<sup>28</sup> For instance, Schlee *et al.* used a mixture of lignin, polyethylene oxide (PEO), and NaNO<sub>3</sub>/NaOH to electrospin free-standing carbon EDLC.<sup>27</sup> These CFMs achieved 195 F g<sup>-1</sup> and 350 mF cm<sup>-2</sup> at 0.1 A g<sup>-1</sup> (6M KOH, 1.2 V window) with the performance decreasing by only 15%–30% when the current was increased to 100 A g<sup>-1</sup>. An alternative approach enhancing electrochemical performance is to incorporate pseudocapacitive materials, such as MnO<sub>2</sub>,<sup>29,30</sup> MoS<sub>2</sub>,<sup>31</sup> SnO<sub>2</sub>,<sup>32</sup> and Fe<sub>2</sub>O<sub>3</sub>,<sup>33</sup> onto the surface or into the carbon fibers. For instance, Kim *et al.* electroplated and then hydrothermally synthesized NiGa<sub>2</sub>S<sub>4</sub> onto the surface of electrospun polyacrylonitrile (PAN) carbon fibers to improve the energy density of the flexible fibers and increase the conductivity of NiGa<sub>2</sub>S<sub>4</sub>.<sup>17</sup> This combination attained an energy density of 41 Wh kg<sup>-1</sup> at a power density of 0.6 W kg<sup>-1</sup> and displayed a minimal change in performance when bent around a metal rod, indicating the exceptional flexibility and conductivity afforded from the carbon fibers.

These studies were important first steps in improving the electrochemical performance. However, increasing the porosity using

templates and activation agents tends to come at the expense of mechanical properties (e.g., strength and flexibility) as the carbon fiber structure is broken/interrupted by the formation of pores. Thus, one of the main challenges moving forward for CFMs is how to improve the performance while maintaining the mechanical properties that set them apart from powdered supercapacitors. Recently, Ramachandran *et al.* demonstrated an interesting approach to this problem by manipulating the phase separation behavior of different polymer blends to create porous carbon fibers with improved mechanical strength via gel-spinning.<sup>34</sup> Fibers created from a blend of polyacrylonitrile (90%) with poly (acrylic acid) (10%) had a tensile strength/modulus of 1.7/287 GPa, which compared favorably to polyacrylonitrile fibers (1.9/251 GPa). The pores in these fibers were oriented along the fiber axis, which did not interfere with the graphitic order in the fiber, leading to increased strength. A recent review on the mechanical properties of electrospun fibers highlighted the key issues within the field, namely, the absence of standardized testing and failure mechanism studies and the difficulty in measuring single fibers. These points need to be addressed to realize the objective of high strength, high capacitance, carbon fiber supercapacitors.

Future enhancements in the properties of CFMs are likely to also come from the development of composite fibers and advanced fiber architectures. Coaxial spinning, where different polymer solutions are combined at the needle tip to create novel core-sheath and hollow morphologies, has shown significant promise.<sup>35</sup> For instance, Xiao *et al.* created porous hollow carbon fibers by using paraffin oil as the core and PAN mixed with the hard template tetraethyl orthosilicate as the sheath.<sup>24</sup> These CFM exhibited a performance of 261 F g<sup>-1</sup> in 3M KOH (1 A g<sup>-1</sup>, 1 V, three electrode) and 48 F g<sup>-1</sup> in EMIMBF<sub>4</sub> (1 A g<sup>-1</sup>, 2.5 V, two electrode). More importantly, folding the electrode over 1000 times to 180° lowered the capacitance by only 2%, demonstrating the exceptional electrochemical performance under deformation of CFMs. The next step for coaxial spinning will be to incorporate pseudocapacitive materials onto the outside of the fibers while maintaining a strong carbon fiber core. This step would eliminate the need for post-spinning doping and simplify the process. However, there are several challenges that need to be overcome when coaxially spinning pseudocapacitive materials and polymeric carbon fiber precursors. First, an adequate bond is needed between the pseudocapacitive material and the carbon fiber. This bond is important to increase the conductivity of the pseudocapacitive material and ensure that it does not delaminate from the carbon fiber. Second, the thermal stability of the pseudocapacitive material needs to be higher than the carbonization temperature for forming the carbon fiber. Finally, fundamental studies understanding how the morphology of these fibers influences the performance is also needed.

Sustainability is another challenge for CFMs. The majority of CFMs reported in the literature and produced industrially are based on petroleum derived polymers, such as polyacrylonitrile (PAN),<sup>23,30,33,36–38</sup> poly(methyl methacrylate) (PMMA),<sup>33,36–38</sup> and polyvinyl pyrrolidone (PVP).<sup>36,39–41</sup> To improve the sustainability of CFMs, alternatives to these polymers have become a hot topic. One of the leading candidates is lignin, a complex 3D organic polymer extracted from lignocellulosic biomass and extracted during pulp and paper production. To electrospin, lignin is typically

combined with other polymers to enhance its ability to form carbon fibers. For instance, Zhu *et al.* combined fractionated corn stalk lignin with PAN (1:1) and electrospun CFMs that were chemically activated with KOH to increase the porosity.<sup>42</sup> These CFMs achieved a high energy density of 37.1 Wh kg<sup>-1</sup> at 400 W kg<sup>-1</sup> and maintained an energy density of 28.4 Wh kg<sup>-1</sup> at a power density as high as 8 kW kg<sup>-1</sup> (6M KOH, 1 V window). However, to make these materials truly sustainable, the petroleum-based polymers need to be completely replaced. Yang *et al.* replaced the polymer with naturally occurring proteins that were subsequently mixed with lignin and electrospun.<sup>43</sup> At a ratio of 50/50, lignin to protein was found to be stable under 900 °C, forming a self-standing flexible carbon fiber mat that was subsequently activated with CO<sub>2</sub> at 850 °C. These fibers achieved a specific capacitance of 360 F g<sup>-1</sup> (1 A g<sup>-1</sup>, 6M KOH, 1 V window); however, they were not tested as a free-standing electrode, suggesting that it is unstable under electrochemical testing. Thus, there is significant scope to further develop natural polymers for the manufacturing of CFMs to enhance their sustainability.

A final key challenge is the limited production capacity of traditional single-needle electrospinning (0.1–1 g h<sup>-1</sup>) commonly deployed in the literature. Multi-needle setups have been used to increase the throughput, but suffer issues with electrostatic repulsion, needle clogging, and a lower level of quality control. Two potential alternatives have been identified to enhance CFM production: (a) needleless electrospinning and (b) centrifugal electrospinning. In needleless electrospinning, a thin layer of polymer is coated onto an open surface, such as a cylinder, disk, ball, spiral coil, bowl, or mushroom,<sup>44</sup> and rotated to form multiple conical spikes on the surface of the solution.<sup>45</sup> Applying a potential converts these spikes into Taylor cones and ultimately the polymer jets that form carbon fibers. Due to the high number of Taylor cones that can be created, needleless electrospinning has a higher throughput than needle-based electrospinning. However, the following drawbacks need to be overcome: (a) the high potential (50–100 kV) needed to form the Taylor cones vs needle-based spinning (10–25 kV), (b) limited control of fiber morphology, and (c) difficulty in creating coaxial fibers.<sup>46</sup>

Centrifugal spinning uses a high-speed spinneret to exert a centrifugal force on the polymer solution, creating a liquid jet that is then stretched into fibers.<sup>20</sup> The process is simple and has a high production throughput and good fiber alignment. When combined with electrospinning, the morphology of the fibers is enhanced, and nano-sized CFMs are achievable. For instance, Zheng *et al.* centrifugally electrospun a mixture of PAN and polyethylene glycol forming nanosized fibers that had a 400% higher tensile strength than the purely electrospun fibers.<sup>47</sup> These CFMs also exhibited a specific capacitance of 277 F g<sup>-1</sup> (0.2 A g<sup>-1</sup>, 1M H<sub>2</sub>SO<sub>4</sub>, 1 V window), negligible difference in the cycling voltammetry curve when bent to 180°, and 8.18 Wh kg<sup>-1</sup> energy density at 4.27 kW kg<sup>-1</sup> power density. As with needleless electrospinning, centrifugal electrospinning is still in its early stages, and further studies are needed to understand how the spinning parameters influence the final fiber properties.

With intrinsic flexibility, conductivity, electrical double layer capacitance, and dopability to introduce pseudocapacitance, along with the ability to eliminate binders, conductive agents, and

current collectors, CFMs are the next step in flexible supercapacitors and energy storage. Although our understanding of electrospinning and developing CFMs with novel morphologies and properties are improving, we are still in the nascent stage of CFM development

for supercapacitors. Improvements to sustainability, performance, manufacturing, and understanding the structural significance for mechanical properties are vital to driving this promising technology forward (Fig. 1).

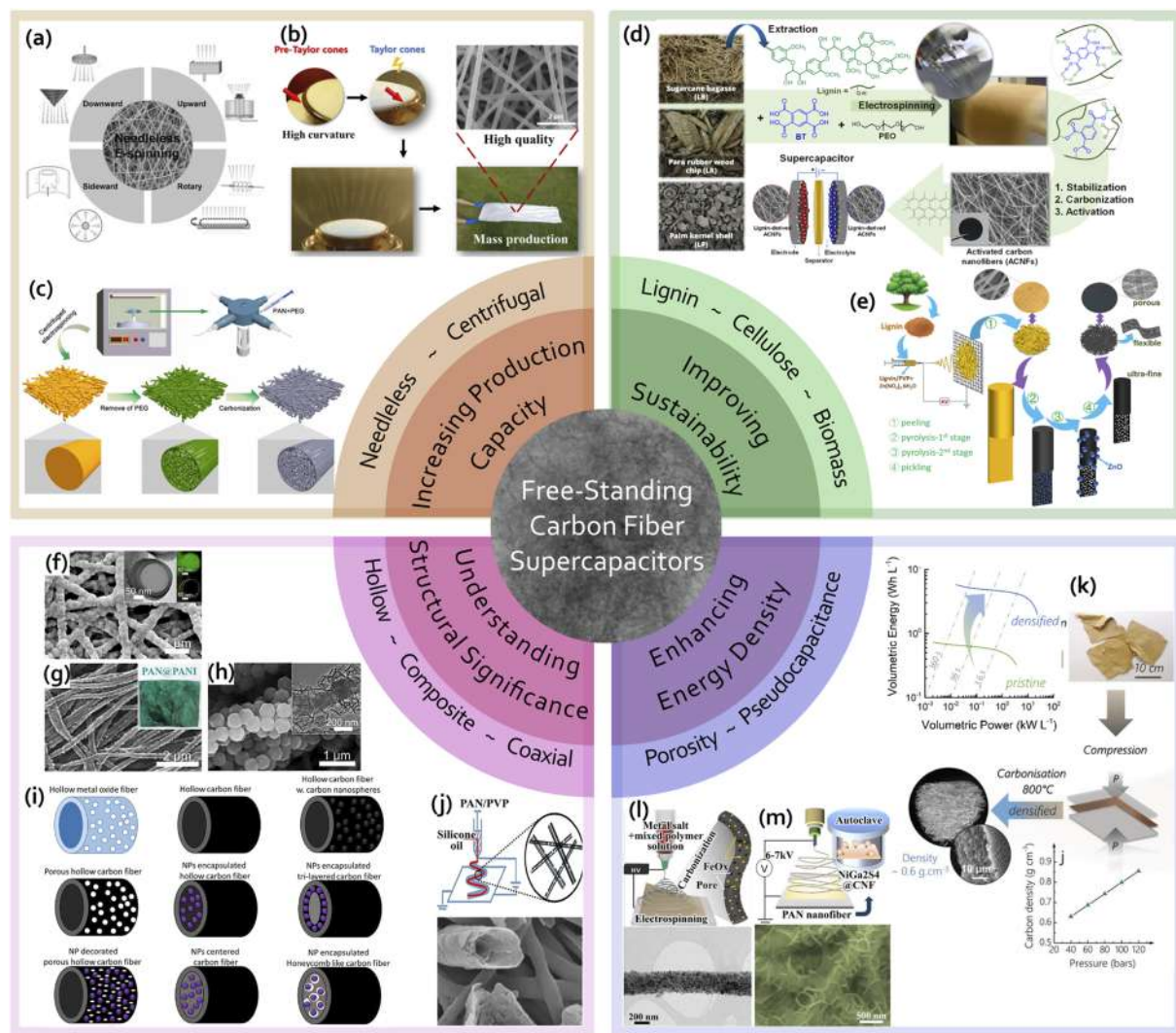


**FIG. 1.** Future key areas for the advancement of free standing supercapacitors with current examples from the literature. (a) Examples of needleless electrospinning setups. Reproduced with permission from Yu *et al.*, *Macromol. Mater. Eng.* **302**(7), 1700002 (2017).<sup>45</sup> Copyright 2017 John Wiley & Sons. (b) Novel mushroom spinneret for needleless electrospinning. Reproduced with permission from Xiong *et al.*, *Mater. Des.* **197**, 109247 (2021).<sup>44</sup> Copyright 2021 Elsevier. (c) Nano-channel carbon fibers created from centrifugal electrospinning. Reproduced with permission from Zheng *et al.*, *Microporous Mesoporous Mater.* **316**, 110972 (2021).<sup>47</sup> Copyright 2021 Elsevier. (d) Lignin-based carbon fiber supercapacitors from different lignin sources. Reprinted with permission from Khamnantha *et al.*, *ACS Appl. Nano Mater.* **4**(12), 13099–13111 (2021).<sup>48</sup> Copyright 2021 American Chemical Society. (e) ZnO-assisted synthesis of microporous lignin carbon fibers. Reproduced with permission from Ma *et al.*, *J. Colloid Interface Sci.* **586**, 412–422 (2021).<sup>49</sup> Copyright 2021 Elsevier. (f) Silver plated carbon nanofibers. Reproduced with permission from Kim *et al.*, *Chem. Eng. J.* **353**, 189–196 (2018).<sup>50</sup> Copyright 2018 Elsevier. (g) Electrospun polyacrylonitrile@polyaniline core-shell nanofibers. Reproduced with permission from Miao *et al.*, *Electrochim. Acta* **176**, 293–300 (2015).<sup>51</sup> Copyright 2015 Elsevier. (h) Manganese-doped zinc oxide carbon nanofibers. Reproduced with permission from Samuel *et al.*, *Chem. Eng. J.* **371**, 657–665 (2019).<sup>52</sup> Copyright 2019 Elsevier. (i) Possible fiber architectures for energy storage using coaxial electrospinning. Reproduced with permission from D. Han and A. J. Steckl, *ChemPlusChem* **84**(10), 1453–1497 (2019).<sup>35</sup> Copyright 2019 John Wiley & Sons. (j) Hollow-porous carbon fibers. Reproduced with permission from He *et al.*, *Electrochim. Acta* **222**, 1120–1127 (2016).<sup>25</sup> Copyright 2016 Elsevier. (k) Densification of lignin carbon fibers to enhance volumetric density. Reproduced with permission from Hérou *et al.*, *Adv. Sci.* **8**(17), 2170109 (2021).<sup>53</sup> Copyright 2021 Author(s), licensed under a Creative Commons Attribution 4.0 License. (l) Carbon nanofibers decorated with FeO nanoparticles. Reproduced with permission from Samuel *et al.*, *Chem. Eng. J.* **328**, 776–784 (2017).<sup>54</sup> Copyright 2017 Elsevier. (m) Carbon nanofibers decorated with NiGa<sub>2</sub>S<sub>4</sub>. Reproduced with permission from Kim *et al.*, *Chem. Eng. J.* **420**, 130497 (2021).<sup>17</sup> Copyright 2021 Elsevier.

### B. 3D printed free-standing supercapacitor components

3D printing, also known as additive manufacturing, is an alternative to spinning methods for fabricating the components of free-standing supercapacitors.<sup>55–59</sup> The ability of 3D printing to generate a wide range of functional 3D structures with complex geometries allows for facile freeform fabrication and rapid prototyping with a minimal usage of materials and low cost. So far, different 3D printing techniques, such as laser-, lithography-, and extrusion-based methods, have been applied for the preparation of single free-standing carbon or pseudocapacitive material-based electrodes for supercapacitors.<sup>60,61</sup> Based on the type of fabrication, they can

be broadly classified into direct 3D printing, 3D printing combined with pyrolysis, and hybrid approaches (Fig. 2).

Direct 3D printing is a single-step approach that allows for direct construction of 3D printed electrodes, providing high flexibility for the creation of complex architectures via non-contact fabrication processes.<sup>62</sup> Fused filament fabrication (FFF) or fused deposition modeling (FDM) [Figs. 2(c) and 2(d)], inkjet printing (IJP) [Figs. 2(e)–2(g)], and direct-ink writing (DIW) [Figs. 2(h)–2(k)] (also known as robocasting) are the most used extrusion-based 3D printing processes.<sup>57,59,63</sup> To fabricate the different components of supercapacitors with these methods, inks are commonly prepared by suspending carbon-based materials, such as activated carbon

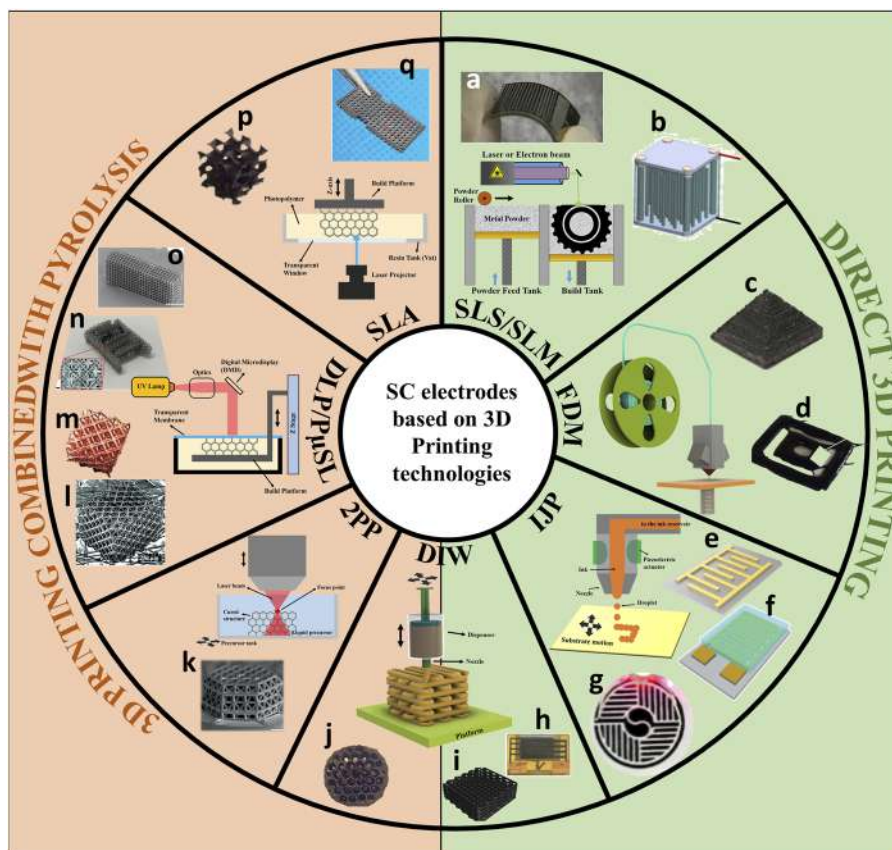


**FIG. 2.** Schematic illustrating the various supercapacitor electrodes fabricated based on 3D printing technologies. (a) Selective laser sintering (SLS). Reproduced with permission from He *et al.*, *Carbon* **161**, 117–122 (2020).<sup>75</sup> Copyright 2020 Elsevier. (b) Selective laser melting (SLM). Reproduced with permission from Zhao *et al.*, *Electrochem. Commun.* **41**, 20–23 (2014).<sup>76</sup> Copyright 2014 Elsevier. (c) Reproduced with permission from Zhang *et al.*, *Synth. Met.* **217**, 79–86 (2016).<sup>77</sup> Copyright 2016 Elsevier. (d) Reproduced with permission from Areir *et al.*, *J. Manuf. Process.* **25**, 351–356 (2017).<sup>78</sup> Copyright 2017 Elsevier. Fused deposition modeling (FDM). (e) Reproduced with permission from Wang *et al.*, *Energy Storage Mater.* **36**, 318–325 (2021).<sup>79</sup> Copyright 2021 Elsevier B.V. (f) Reproduced with permission from Liu *et al.*, *J. Mater. Chem. A* **4**(10), 3754–3764 (2016).<sup>80</sup> Copyright 2016 Royal Society of Chemistry. (g) Reproduced with permission from Choi *et al.*, *Energy Environ. Sci.* **9**(9), 2812–2821 (2016).<sup>81</sup> Copyright 2016 RSC Publishing. Ink jet printing (IJP). (h) Reproduced with permission from Liu *et al.*, *Adv. Funct. Mater.* **28**(21), 1706592 (2018).<sup>82</sup> Copyright 2018 John Wiley & Sons. (i) Reproduced with permission from Yao *et al.*, *Joule* **3**(2), 459–470 (2019).<sup>86</sup> Copyright 2019 Elsevier. (j) Unpublished work DTU Nanolab Direct ink writing (DIW). (k) 2 photon polymerization (2PP). Reproduced with permission from Bauer *et al.*, *Nat. Mater.* **15**(4), 438–443 (2016).<sup>83</sup> Copyright 2016 Springer Nature. (l) Projection micro-stereolithography (PμSL).<sup>84</sup> (m) Reproduced with permission from Xue *et al.*, *Nano-Micro Lett.* **11**(1), 46 (2019).<sup>85</sup> Copyright 2019 Springer Nature. (n) Reproduced with permission from Park *et al.*, *Langmuir* **34**(37), 10897–10904 (2018).<sup>86</sup> Copyright 2018 American Chemical Society. (o) Digital light processing (DLP). Reproduced with permission from Narita *et al.*, *Adv. Energy Mater.* **11**(5), 2002637 (2020).<sup>87</sup> Copyright 2020 John Wiley & Sons. (p) Stereolithography (SLA).<sup>72</sup> (q) Reproduced with permission from Wang *et al.*, *Adv. Mater. Technol.* **5**(6), 1901030 (2020).<sup>88</sup> Copyright 2020 John Wiley & Sons, Inc. All rights reserved.

(AC), graphene,<sup>64</sup> carbon nanotubes (CNTs), or MXene,<sup>65</sup> for electrodes or dissolving polymeric, colloidal, or poly-electrolyte building blocks for electrolytes into a liquid.<sup>57,60</sup> For example, Yao *et al.* printed a 3D scaffold containing graphene oxide (GO) that was loaded with MnO<sub>2</sub>, achieving a specific capacitance of 187.2 F g<sup>-1</sup> (10 mA cm<sup>-1</sup>, 0.8 V window, 3M LiCl).<sup>66</sup> Additionally, increasing the electrode thickness led to an increase in areal capacitance with no loss of gravimetric capacitance, demonstrating that larger electrodes can be printed without loss in performance.

A major challenge of extrusion-based 3D printing is its resolution as the material used for preparing the ink tends to agglomerate and clog the nozzle.<sup>67</sup> This issue results in larger nozzles for printing, limiting the resolution of these 3D printed electrodes. Thus, future advancements in this field will come from the development of new printable inks and identifying their optimal printing parameters. To achieve this, first, the viscoelastic properties of the inks need to be optimized to allow flow through the nozzle and achieve printing through extrusion. For example, for inkjet printing, liquid inks with low viscosity are usually used to create thin films or patterns with uniform thickness as they can quickly form droplets and deposit on the building platform.<sup>68</sup> Second, the ink should have sufficient mechanical strength to support the entire 3D structure during the ink deposition and rapid solidification processes post-printing. Thus, it is crucial to have good control of ink formulations and rheological properties to generate a stable dispersion that promotes the fluid-to-gel transition for shape retention after printing. Ideally, an open-source library of printable ink formulations is needed to accelerate the development of extrusion-based 3D printing techniques.

An alternative solution to the limited resolution of extrusion-based 3D printing is using lithography techniques to create 3D polymer structures that are subsequently pyrolyzed at high temperatures. This type of 3D printing generally creates 3D structures in a layer-by-layer fashion by using photo-polymerization to solidify each layer of light-sensitive resins, with resolution depending on the type of UV source and the material [Fig. 2(l)]. Recent developments in this field with the introduction of projection micro-stereolithography (PμSL) have enabled the creation of features as small as 2 μm [Figs. 2(m)–2(o)].<sup>69,70</sup> Although lithography-based 3D printing techniques can fabricate polymer-based 3D structures with complex shapes and high resolution, the obtained carbon structures do not immediately possess good electrochemical performance.<sup>71</sup> To overcome this limitation, Rezaei *et al.* used stereolithography (SLA) followed by pyrolysis to create complex 3D pyrolytic carbon electrodes [Figs. 2(p) and 2(q)].<sup>71</sup> They found that directly pyrolyzing at 10 °C min<sup>-1</sup> resulted in a 31% lower charge transfer resistance than the one obtained with a two-step approach, indicating the importance of pyrolysis conditions for this technique.

Similar to CFMs, additional electrochemical performance can be achieved through the incorporation of pseudocapacitive materials onto the surface of the 3D printed electrode. For example, Mn<sub>3</sub>O<sub>4</sub> nanostructures added to a 3D printed microporous architecture lead to a gravimetric capacitance of 186 F g<sup>-1</sup> and an aerial capacitance of 968 mF cm<sup>-2</sup> (0.5 mA g<sup>-1</sup>, 1.1 V window, 1M H<sub>2</sub>SO<sub>4</sub>).<sup>72</sup> Future developments in this field are likely to come from modifying the resin by adding sacrificial or hard templates to increase the porosity and conductive polymers to enhance the conductivity and pseudocapacitive materials.

Realistically, the ultimate goal for 3D printed supercapacitors from an industrial perspective is to 3D print an entire supercapacitor device. This is unlikely to be achieved with a single printing method, and as such, the benefits of different 3D printing techniques could be combined to create each component. For instance, lithography could be used to build the electrode structure, while extrusion-based 3D printing could add pseudocapacitive materials to the surface and the electrolyte.

Another crucial step is improving the sustainability of 3D printing through the manipulation of biomass-derived carbon materials. These materials are well known for their hierarchical porous structure, which is highly beneficial as electrodes for supercapacitors.<sup>73,74</sup> However, no works have yet been reported fabricating 3D structured electrodes using biomass for supercapacitor application. One way to fabricate 3D structured free-standing electrodes from biomass is to exploit direct ink writing by using inks prepared from biomass materials [Fig. 2(j), unpublished work DTU Nanolab]. As these organic materials are non-conductive, a high temperature pyrolysis, laser, or microwave irradiation is required to convert them into conductive 3D carbon for supercapacitors, which can further tailor the properties of these materials. This combined approach of biomass, 3D printing, and carbonization is in its nascent stage and will likely bring exciting new sustainable possibilities to 3D printed supercapacitors.

Another approach that could be exploited is to use the hybrid technique reported by Pan *et al.*<sup>89</sup> where conventional UV photolithography and stereolithography-based 3D printing are combined to obtain high aspect ratio 3D structures that are otherwise impossible to fabricate by conventional photolithography alone. Combining this hybrid technique with wet or electrochemical deposition of electroactive materials could be utilized to fabricate on-chip supercapacitor devices.<sup>90</sup> Moreover, by replacing SLA-based 3D printing with PμSL, electrodes with much higher resolution and aspect ratios could be fabricated. This would help to achieve optimal use of the vertical dimension by increasing the active materials without increasing the footprint area and dramatically improve the volumetric capacitance, energy, and power density of the supercapacitor device.

Overall, 3D printing allows for the manufacturing of free-standing 3D-printed electrode architectures with well-defined morphologies, diverse features, and a high degree of design freedom. Moreover, it provides the ability to create high aspect ratio structures with optimal use of the vertical dimension, which are simply not possible using conventional slurry-based fabrication. As a result, 3D printed architectures will continue to emerge and establish a significant and pervasive impact on supercapacitors.

### C. Electrolytes for free-standing supercapacitors

To fully exploit the advantages of free-standing supercapacitors, the electrolyte needs to be more than just an ionic conductor. Ideally, it should impart mechanical strength while maintaining high ionic conductivity, provide excellent contact between the electrode and the electrolyte, and have high stability. Many of the studies in powdered and free-standing supercapacitors use aqueous KOH electrolytes to demonstrate the performance of their materials. This is due to its inherently high ionic conductivity, leading to higher capacitances than many other aqueous electrolytes. Thus, it has

become a pseudo-benchmark electrolyte for EDLC studies. However, KOH electrolytes are not necessarily suitable for free-standing applications due to their small voltage window (1–1.2 V), highly corrosive nature, and safety risks around leaking. Recently, hybrid electrolytes have emerged as a possible solution achieving these objectives. These electrolytes are synergistic mixtures of compounds (e.g., polyvinyl acetate/H<sub>2</sub>SO<sub>4</sub>) that result in expanded voltage windows, ionic conductivity, stability, and, most importantly for free-standing supercapacitors, improved mechanical properties. Quasi-solid-state polymer gel electrolytes are the most employed hybrid electrolytes used in free-standing capacitors, comprising a liquid electrolyte entangled in a host polymer.<sup>91</sup> The electrolytes with the highest capacitance so far are aqueous/polymer mixtures, with 563.7 F g<sup>-1</sup> (0.5 A g<sup>-1</sup>, 1 V) being achieved using a H<sub>2</sub>SO<sub>4</sub>/polyvinyl acetate.<sup>92</sup> However, aqueous electrolytes are restricted to a voltage window of ~1.2 V, limiting the energy density. Alternatively, 442.3 F g<sup>-1</sup> (5 mA cm<sup>-2</sup>) was achieved with an organic PVDF-PC-Mg(ClO<sub>4</sub>)<sub>2</sub>-SiO<sub>2</sub> as the electrolyte in an expanded 2 V window.<sup>93</sup>

One of the main challenges for polymer gel electrolytes is achieving a high contact area between the electrode surface and the electrolyte. Ensuring that the polymer permeates into the pores of the electrode is critical for achieving high capacitance and minimizing the equivalent series resistance. Additionally, the thickness of the polymer electrolyte should be kept to a minimum to improve the ionic conductivity. This is where 3D printing is likely to excel over casting methods as gel electrolytes could be mixed at the print head to enable them to easily permeate into the pores before quickly solidifying to form the gel-electrolyte.

Future developments in electrolytes are also likely to come from the incorporation of additives into the electrolyte matrix. For instance, adding redox active species to the electrolyte creates redox couples on the electrode surface that increase the capacitance of the supercapacitor, improving the overall energy density. Sun *et al.* added Na<sub>2</sub>MoO<sub>4</sub> to H<sub>2</sub>SO<sub>4</sub> and achieved 841 F g<sup>-1</sup> (1.8 V window) on activated carbon electrodes.<sup>94</sup> However, cycle stability and self-discharge are major challenges for these electrolytes. An alternative approach is to incorporate liquid crystals into the electrolyte to combat the self-discharge and leakage current behavior of supercapacitors, which prevents them from storing charge over prolonged periods of time. For instance, Xia *et al.* reported a 80% reduction in the leakage current by adding the liquid crystal 2% 4-*n*-pentyl-4'-cyanobiphenyl (5CB) to 1M triethylmethylammonium tetrafluoroborate (TEMABF<sub>4</sub>) in acetonitrile electrolyte. The incorporation of the liquid crystal increased the electrolytes viscosity, slowing the diffusion on ions and self-discharge as a result. Overall, understanding how these electrolytes work to enhance the performance of supercapacitor systems is key to unlocking their potential.<sup>95</sup>

### III. FUTURE APPLICATIONS FOR FREE-STANDING SUPERCAPACITORS

#### A. Wearable free-standing supercapacitors

Distributed sensors in body-area networks for motion sensing in sportswear and point of care diagnostics for healthcare require local energy supply to power sensors on demand. Wearable energy nanogenerators can be integrated into clothing; however,

their supplied energy is not constant and uniform. Thus, wearable supercapacitors built on free-standing and flexible materials and integrated into textiles promise to deliver the required energy supply when needed.<sup>96</sup> After being incorporated into the fabrics, free-standing supercapacitors can power other small electrical devices, such as a simple light-emitting-diode (LED)<sup>97,98</sup> and a cable-type sensor and transistor,<sup>98</sup> and store energy harvested by energy converters, such as solar cells<sup>99</sup> and nanogenerators,<sup>100</sup> enhancing the feasibility of various electronic devices' wearable applications.<sup>101</sup> Compared with standard commercial supercapacitors, wearable supercapacitors need to be lightweight, flexible, safe for humans and the environment, and stable and have a long life. To move from the laboratory to commercial production, wearable supercapacitors still need further improvements on their electrochemical and mechanical performance to become suitable for large scale manufacturing.

Wearable supercapacitors can be designed as thin-film supercapacitors or fiber-shaped supercapacitors. Thin-film supercapacitors are normally composed of conductive flexible planar substrates as electrodes and solid electrolytes with separator layers.<sup>96</sup> For wearable applications, which need devices to be flexible and lightweight, commonly used metal electrodes are not suitable due to their rigid nature.<sup>102</sup> New materials, such as graphene, graphene oxide (GO),<sup>103,104</sup> reduced GO (rGO), and MXenes,<sup>105</sup> have demonstrated suitable electrical and mechanical properties for highly flexible textile and fiber-based supercapacitors,<sup>106</sup> while semiconducting Transition Metal Dichalcogenides (TMDs), such as molybdenum disulfide (MoS<sub>2</sub>)<sup>107</sup> or molybdenum diselenides (MoSe<sub>2</sub>), are semiconducting 2D materials suitable for wearable and textile electronics (Table 1).<sup>64,108</sup> Through dip-coating or vacuum filtration through membranes, these materials can be combined with flexible substrates, including cotton/carbon fabrics, papers, and plastic substrates, such as polyaniline (PANI), polypyrrole (PPy), and polythiophene (PT) sheets,<sup>109</sup> resulting in films or textiles with high tensile strength and relatively low Young's modulus [Fig. 3(a)].<sup>98,101</sup> Besides the mechanical strength, the high stretchability and elasticity of the devices are significant in wearable applications. To maximize these material properties, efforts were made modifying the geometrical design of the substrates. Wrinkled structures or gaps were introduced to the substrate surfaces to enhance the substrate strength during bending or stretching [Fig. 3(b)]. Compared with simple reliance on the stretchability of the material, strengthening from modification of the configuration could minimize the negative influence on electrochemical performance during bending or stretching. From an industrial perspective, it would be ideal if these materials could be integrated in a single step into the spun textile fiber. Electrospinning offers this possibility; however, the mechanical properties of electrospun carbon fibers still need to be enhanced.

Considering the comfort during wearing, single fiber-shaped supercapacitors have been developed, which have a higher degree of flexibility to be woven into the textile together with other electrical devices. The fiber-shaped supercapacitor structure can be a parallel fiber arrangement (use two electrode fibers placed in parallel or twisted with each other) or a coaxial arrangement.<sup>112</sup> In the first configuration, two fibers were used as electrodes and separated by a solid or gel electrolyte around them, and in the second one, a single fiber was built with an inner core electrode fiber and an outer electrode



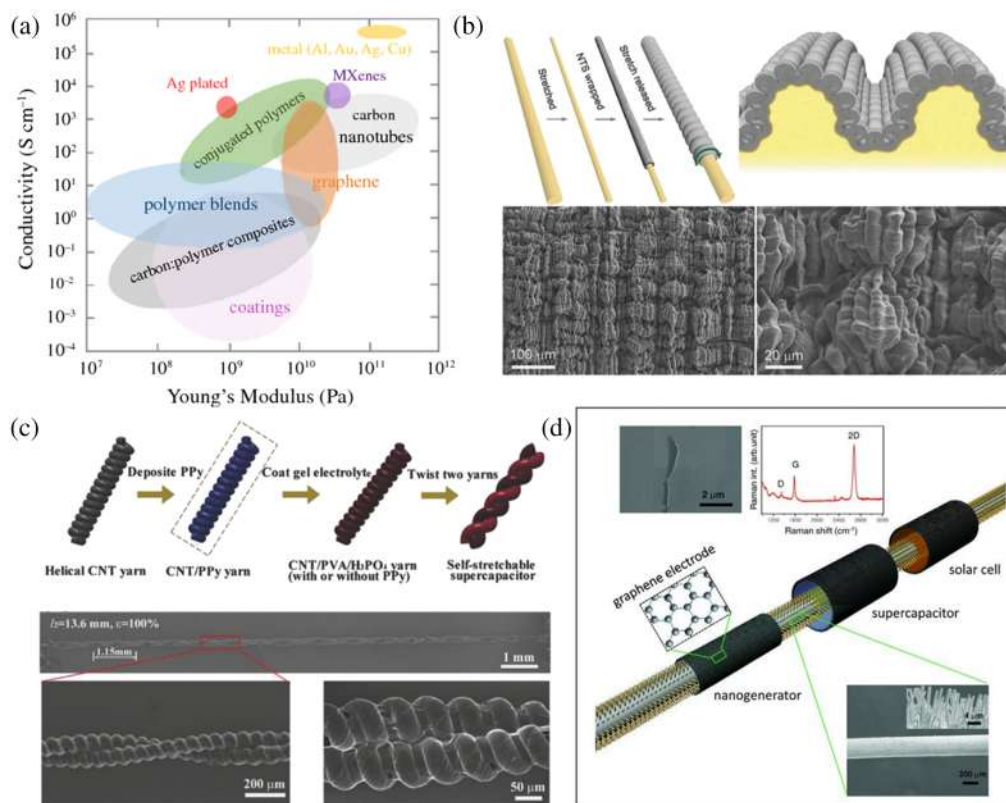


**FIG. 3.** (a) Volume electrical conductivity as a function of Young's modulus for electrically conducting fibers or yarns.<sup>122</sup> (b) Stretchable fibers for energy storage. Reproduced with permission from Liu *et al.*, *Adv. Mater.* **29**(1), 1603436 (2017).<sup>123</sup> Copyright 2017 John Wiley & Sons. (c) Elastic fiber supercapacitors for wearable energy storage. Reproduced with permission from Qin *et al.*, *Macromol. Rapid Commun.* **39**(13), 1800103 (2018). Copyright 2018 John Wiley & Sons. (d) Single-fiber-based hybridization of energy converters and storage units using graphene as electrodes. Reproduced with permission from Bae *et al.*, *Adv. Mater.* **23**(30), 3446–3449 (2011). Copyright 2011 John Wiley & Sons.

shell separated by a solid or gel electrolyte. Compared with the parallel arrangement, the coaxial arrangement ensures a more reliable insulation layer between the two electrodes, especially during the twisting and bending in the wearing process. A coaxial fiber-shaped supercapacitor provides typically a larger active area than a parallel arranged one.<sup>113</sup>

The size of a fiber-shaped supercapacitor is usually between a few micrometers and millimeters.<sup>96</sup> To make these small electric

devices meet the electrochemical and mechanical demands in wearable applications, efforts were made to develop suitable materials and reliable fabrication techniques. Like thin-film supercapacitors, 2D materials, conductive polymers, and transition metal oxides were commonly used in a fiber-shaped supercapacitor due to their high electrical conductivity and flexibility. Moreover, fiber integration processes, such as weaving or knitting, require mechanical flexibility. Using conductive stretchable fiber substrates, such as elastic polymer fibers, metal nanowires, and carbon materials, such as rGO or CNT fibers, is a straightforward way to overcome the problem. Besides adjustment to the materials, modification to the structure also strengthens the fiber. Through the modification of the supercapacitor configuration, Shang *et al.* used a single twisted helical structure fiber configuration to successfully design a fiber-shaped supercapacitor with tensile strains of up to 285% [Fig. 3(c)].<sup>114</sup> A similar structure was applied by Ren *et al.* to build a stretchable fiber-shaped supercapacitor based on two coiled CNT yarns, which showed a specific volumetric capacitance of  $18.12\ F\ cm^{-3}$  and kept a 90% capacitance under 100% strain.<sup>115</sup> These spring-shaped electrodes, also used by Zhang *et al.*, were covered by gel electrolytes,

**TABLE I.** Examples of capacitance of supercapacitors with 2D material electrodes.

Electrode materials	Electrolyte material	Specific capacitance	References
Graphene/GO	KCl	$135\ F\ g^{-1}$	110
rGO	PVA/H <sub>3</sub> PO <sub>4</sub>	$304.5\ F\ cm^{-2}$	111
MXene (Ti <sub>3</sub> C <sub>2</sub> T <sub>x</sub> )	PVA/KOH	$530\ F\ cm^{-3}$	105
1T-MoS <sub>2</sub>	K <sub>2</sub> SO <sub>4</sub> /KBr/KCl	$700\ F\ cm^{-3}$	107

resulting in a fiber-shaped supercapacitor that could be stretched over 300% and kept over 90% specific capacitance under 100% stretching.<sup>116</sup>

As an energy storage unit, a supercapacitor can be used to charge other wearable devices and store the energy from a wearable energy system. Combination with energy harvesting devices is a significant region for wearable supercapacitors to develop and build up a wearable self-powered system in the future. By integrating with solar cells or nanogenerators, wearable supercapacitors can collect solar energy and mechanical energy during daily wearing. Fiber-shaped solar cells can transfer solar energy to electrical energy and then store it as chemical energy in supercapacitors. The energy stored in the supercapacitors can then be used as an energy source for other wearable electric devices. CNT/TiO<sub>2</sub> fibers were wound together with fractional decoration of light-sensitive dye N719 and electrolyte to build a solar cell and a supercapacitor on a single fiber.<sup>99</sup> Eight of these supercapacitors with a specific capacitance of 0.6 mF cm<sup>-2</sup> can be woven together and light an light-emitting diode (LED) on textile. To increase the capacitance and energy conversion, a polyaniline (PANI) coated stainless steel wire was used as the electrodes instead of CNT yarn, which increased the specific capacitance to 19 mF cm<sup>-2</sup>.<sup>97</sup>

Besides solar cells, a nanogenerator is another applied wearable energy convertor, which can convert mechanical energy to electrical energy and store it in supercapacitors. Xiao *et al.* built a coaxial carbon/MnO<sub>2</sub> fiber-shaped supercapacitor linked with a triboelectric generator. This self-powered system could provide the energy output to power a liquid crystal display (LCD) or a LED.<sup>117</sup> The energy convertors can also be integrated together to harvest different types of energies, such as Bae *et al.* integrating a nanogenerator, a solar cell, and a supercapacitor along a single fiber to simultaneously collect mechanical and solar energies [Fig. 3(d)].<sup>118</sup>

Another meaningful wearable application of fiber-shaped supercapacitors is charging sensors on textiles. Through powering the different wearable sensors, various data can be collected and analyzed in real time. One example is the UV photodetector powered by flexible carbon fiber-shaped supercapacitors.<sup>119</sup> After charging the three fiber-shaped supercapacitors connected in series to 3 V, the UV photodetector was powered and showed a change in current in response to UV light. Photodetection can be achieved by Co<sub>3</sub>O<sub>4</sub> coated metal (Ni or Ti)/graphene-coated carbon supercapacitors, where the graphene coating is photoactive and responds to a white light source through a change in leakage current.<sup>120</sup> Flexible supercapacitors can also power strain sensors in wearable applications. Pan *et al.* integrated their coaxial fiber-shaped supercapacitor with a strain sensor and LED.<sup>121</sup> The elastic fiber coated with CNT with MnO<sub>2</sub> or PPy and electrolytes functioned as an asymmetric supercapacitor with a 1.8 V voltage window, which could power a strain sensor coating.

Overall, the development of fiber and textile supercapacitors paves the ways to wearable supercapacitors. Such wearable supercapacitors underpin the generation of wearable self-powered systems and could support various devices, such as personal healthcare (individual management and continuous monitoring of patients), environmental and safety (fire prevention, air, and water quality measurements), and other wearable personal electronics.<sup>101,124</sup>

To this end, textile supercapacitors and fiber-shaped supercapacitors still need further developments to improve performance.

First, compared with common energy units, such as batteries, flexible supercapacitors still show weak points in their energy density. Moreover, improvements in the stretchability and elasticity of the flexible electrodes are necessary steps for both thin-film supercapacitors and fiber-shaped supercapacitors. The best approaches to solve these problems are further developments in flexible electrode materials. Some 2D materials, which are biocompatible, strong in both geometrical directions with electrical conductivity are good choices to build high-performance flexible electrodes for wearable applications. Further improvements can be achieved by developing novel geometrical configurations for wearable supercapacitors. This will not only enhance the mechanical strength and stretchability of the devices but also ensure that their electrochemical performance is retained under bending and stretching.

## B. Free-standing supercapacitors as structural supercapacitors

The laminated architecture and the use of carbon-based electrodes in supercapacitors mirror the architecture of high-performance carbon fiber/polymer composites. These synergies have driven the emergence of structural supercapacitors<sup>125</sup>—electrochemical devices, which have the capacity to bear significant mechanical load.<sup>125–128</sup> This melding of two disparate functions as a multifunctional material is generating considerable academic and industrial interest. By dispensing with the parasitic mass associated with conventional electrochemical devices, free-standing structural supercapacitors can offer huge weight and volume savings<sup>129</sup> and free design constraints in sectors such as electrification of transport,<sup>130</sup> infrastructure, and portable electronics. The development of structural supercapacitors is still relatively immature, and there are still considerable hurdles to be addressed, but the potential to revolutionize future systems is captivating.

First, the constituents for structural supercapacitors must be considered (Fig. 4). Electrodes for structural supercapacitors have used conventional high performance carbon fibers as a backbone,<sup>125</sup> but these materials alone do not offer a sufficient surface area to provide useful electrochemical performance. Therefore, routes to enhance the surface area have included chemical activation and grafting or sizing of nanocarbons, such as carbon nanotubes or graphene, onto the structural fiber surfaces. Such approaches can add modest improvements in capacitance and some enhancement in mechanical performance, particularly matrix-dominated behavior.<sup>125</sup> An alternative has been to surround the structural fibers with a carbon aerogel (Fig. 4),<sup>131</sup> which provides considerable improvements in electrochemical performance (1.12 F g<sup>-1</sup>, 0.80 Wh kg<sup>-1</sup>, 32 W kg<sup>-1</sup> normalized by the full device mass)<sup>132</sup> and mechanically reinforces the matrix space, imparting improvements in mechanical performance.<sup>133</sup> However, carbon aerogel is very brittle and complicates the device manufacturing process. Finally, further strategies have included the introduction of conductive polymers, such as polyaniline, yielding 22 mF g<sup>-1</sup>, 49 mWh kg<sup>-1</sup>, 58 W kg<sup>-1</sup> with a shear modulus of 1.1 GPa and a shear strength of 6.3 MPa,<sup>134</sup> and the adoption of metal oxides or hydroxides to imbue pseudocapacitance.<sup>135–138</sup> The latter has presented significant improvements in electrochemical performance (29 F g<sup>-1</sup>, 0.19 Wh kg<sup>-1</sup>, 37 W kg<sup>-1</sup>) and some apparent enhancement in mechanical performance (Young's modulus of 33 GPa and tensile strength of 489 MPa).

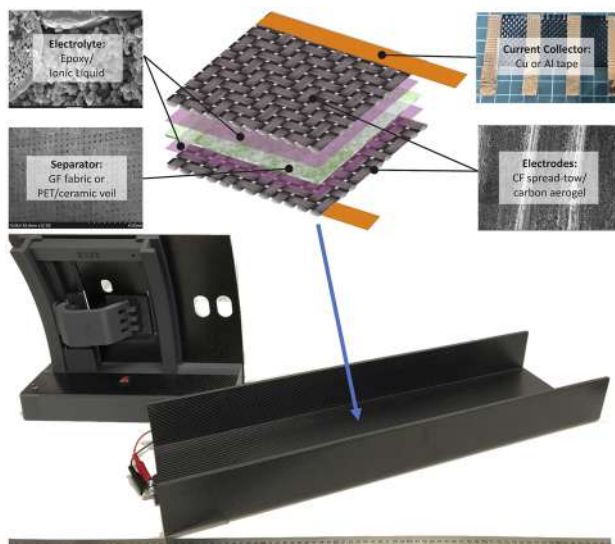


**FIG. 4.** Structural supercapacitor constituents inside a multifunctional fuselage beam demonstrator.

The development of structural electrolytes, on the other hand, is relatively immature because of the considerable challenge of the conflicting requirements of mechanical rigidity and ion transport. The aspiration has been to achieve a Young's modulus exceeding 1 GPa and ionic conductivity over  $0.1 \text{ mS cm}^{-1}$ .<sup>139</sup> Conventional polymer electrolytes are too soft, and therefore, strategies have included (i) homopolymers in which polymer scaffolds are synthesized with structural and ionically conducting phases, which couple mechanical and electrochemical functions;<sup>140,141</sup> (ii) copolymers that decouple these functions where one monomer with sidechains promotes ion conduction and one crosslinking monomer promotes high modulus;<sup>142</sup> (iii) nanocomposites in which nanoparticles or whiskers are introduced into the electrolyte to provide mechanical stiffening; and (iv) gels in which crosslinked structural phases are immiscible with liquid electrolytes, leading to a biphasic structure.<sup>143,144</sup> The latter has been the most successful approach, principally though using epoxy or vinyl ester structural phases with ionic liquids, often with dissolved lithium salts (such as LiTFSI) to supplement the ion concentration.<sup>125</sup>

Regarding the separators, the role is to electrically insulate the electrodes from each other while permitting ion flow between them (Fig. 4). The separator should be chemically inert, porous, and thin to reduce the ion transport distance and tortuosity and to minimize parasitic weight. From a structural perspective, the separator should be robust enough to cope with the processing conditions and stiff/strong to elevate device mechanical performance while forming a strong bond with the electrodes to permit load transfer. Many of the separators used to date have been drawn from conventional electrochemical devices, such as stretched polypropylene (Celgard) membranes, but these polymers suffer from poor mechanical bonding to the electrolyte.<sup>128</sup> Alternatively, cellulose or polymeric non-woven veils and glass fibers (both woven fabric and non-woven veils) have been adopted.<sup>132</sup> These fibrous separators have also presented issues associated with electrolyte compatibility

and loss of ionic conductivity. Novel solutions, such as vertically aligned nano-alumina, have been developed although it is not clear how scalable such processes would be.<sup>145</sup>

Selection and optimization of the current collector (Fig. 4) are critical to the scalability of structural supercapacitors, and using conventional materials (such as copper) can add substantial mass to the device. It is notable that in conventional devices, the electrode is deposited as a powder onto a current collector foil, which can constitute as much as 25% of the device mass, but for structural supercapacitors, such an approach is not optimal.<sup>146</sup> Moreover, depositing the current collector onto the structural electrode offers considerable scope for device mass reduction and optimization.<sup>147</sup> Studies at Imperial<sup>147</sup> have demonstrated that the scale-up of devices from  $0.8$  (Swagelok) to  $446 \text{ cm}^2$  (A4 size) with edge strip current collectors (as used in much of the literature) leads to enormous reductions in electrochemical performance. The specific power fell considerably, from  $2.05$  (Swagelok) to  $0.027 \text{ kW kg}^{-1}$  (A4 size), and only slightly recovered to  $0.066 \text{ kW kg}^{-1}$  when the copper mesh was used. This loss in performance with scale is principally attributed to the resistive losses during current collection, which can be partitioned into in-plane (longitudinal and lateral), out-of-plane, contact (electrode/current collector), and inherent current collector resistances in the device. The former (in-plane) is associated with the in-plane resistivity of the electrode, which is dictated by fiber/fiber contact, while out-of-plane resistivity is associated with electrical conduction through the electrode. Contact resistance between the current collector and the electrode is the dominant source of power dissipation for the devices tested, and predictive studies have shown that considerable performance enhancements can be achieved through optimization of the current collector and reduction in contact resistance. These studies have also shown the importance of pressure on the device during use. Compaction of the device improves the fiber/fiber and current collector/electrode contact, hence reducing the resistivities and, thus, the power losses. However, too much pressure leads to shorting of the electrodes and loss in device performance, indicating the importance of the separator in the device. Although in isolation, such as in a laboratory environment, it is feasible to apply the optimum pressure on the device, when in use, controlling the compaction will be challenging. There is a need to find solutions to maximize the performance of devices, perhaps exploring routes to imbue internal through-thickness compressive stresses in the devices to enhance electrochemical performance. This approach has been used in a recent structural supercapacitor demonstrator (Fig. 4) where a C-section beam representative of a fuselage structural component can provide the power to open and close a scale model of an aircraft passenger door.<sup>148</sup>

The encapsulation electrically isolates the cell from the surrounding structure and systems and protects the cell from the environment (i.e., moisture). The encapsulation material should be light weight and robust enough to cope with the handling and processing conditions. The encapsulation material could contain multiple stacks of cells to minimize the parasitic mass associated with the encapsulation. Encapsulation can account for a sizable proportion of the device mass (i.e., 10%<sup>149</sup>). For structural power devices, there is the additional requirement that the encapsulation material should transmit mechanical loads across the device/encapsulation/system interfaces: none of the conventional encapsulation solutions address this need, so fresh solutions are required.

Overall, structural electrode development is fairly well advanced, with the main challenge being to increase the electrode volume fraction to enhance both mechanical performance (i.e., Young's modulus) and active mass. Generally, to ease processing, woven carbon fiber fabrics have been used, but eventually, unidirectional tapes would be preferable to maximize mechanical performance. For structural electrolytes, although encouraging mechanical and ionic conductivities have been demonstrated in the bulk, challenges arise upon introduction to the reinforcements (electrodes and separator), leading to heterogeneity and loss of the optimal microstructure. Finally, some studies have considered inorganic electrolytes, which have a high modulus but present considerable issues regarding brittleness, interface optimization, and processability. Additionally, several challenges arise when manufacturing large scale multifunctional components for demonstrators that are not encountered when manufacturing single-cell lab-scale devices. The key issues are resistive losses, scale-up, multicell architecture, reproducible manufacture, and complex geometry components. Solutions to these engineering challenges would enable structural power composites to revolutionize structural and electrical engineering applications.

#### IV. SUMMARY AND OUTLOOK

In conclusion, shifting from powdered to free-standing supercapacitor electrodes is now becoming a leading solution to realize new applications and technologies using supercapacitors as their energy source. Challenges in creating fiber mats, 3D printed electrodes, wearable, and structural applications still exist, with specific problems outlined above. However, there are overlapping challenges that also need to be addressed to fully realize the benefits of free-standing supercapacitors.

First, understanding the linkage between mechanical properties and the morphological and physicochemical properties of the electrode or electrolyte is critical in tailoring free-standing supercapacitors toward specific applications. For instance, wearables require highly flexible, lightweight, stretchable, and washable materials, whereas structural supercapacitors require high stiffness, strength, and toughness. Currently, this understanding is hindered by the lack of standardized methods for testing the mechanical properties of these materials. Developing standardized testing regimes will enable easy comparisons between materials developed by different teams.

Second, the performance of free-standing electrodes, whether they are fiber-based or 3D printed, needs to be improved to match the same level as current commercial supercapacitors while maintaining their mechanical advantages. This enhancement is likely to be achieved through the development of complimentary composite materials that exploit the advantages of carbon (e.g., flexibility and conductivity) and pseudocapacitive (e.g., energy density) materials. Ideally, these materials will be combined in single-step synthesis methods (e.g., coaxial) to lower the industrial production cost. Furthermore, directly 3D printing onto carbon fibers is an exciting new possibility for industrially producing free-standing supercapacitors. For example, the flexible carbon fiber mat can act as the base electrode and the current collector, while 3D printing can build on top to add pseudocapacitive materials and the electrolyte.

Third, the utilization of biomaterials for spinning and 3D printing should be examined. Biomaterials contain a range of ordered porous morphologies that are beneficial in improving the electrochemical performance of supercapacitors. For instance, Yu *et al.* demonstrated that carbonized flower petals can be directly utilized as flexible electrodes.<sup>150</sup> Additionally, the use of biomaterials instead of fossil sources for raw materials will improve the sustainability of free-standing supercapacitors and likely reduce their end-of-life impact on the environment.

Fourth, self-discharge and leakage current are issues that prevent supercapacitors from storing charge over long periods of time.<sup>151</sup> Developing strategies to reduce the level of current leakage will enable supercapacitors to be utilized in long term energy storage solutions without the need for batteries.

Finally, the development of electrolytes that enhance the mechanical properties of free-standing supercapacitors is needed. New hybrid electrolytes incorporating different polymers and redox active materials represent an exciting step forward for supercapacitor electrolytes. However, understanding how they interact with the electrode surface using in-operando methods is needed to truly unlock their potential.

Overall, the development of free-standing supercapacitors is a long-term shift in the field, with many challenges remaining before they become commercially available. To a certain extent, the directions mentioned in this Perspective should improve the performance of these materials in the future. However, we have every reason to believe that the unsolved challenges will be addressed through joint efforts as the benefits of free-standing supercapacitors will be the catalyst needed to deliver the next generation of integrated technologies.

#### ACKNOWLEDGMENTS

K.G.L. acknowledges the European Research Council under the Horizon 2020 framework for the Marie Curie Research Fellowship (Grant No. 888124) through the project HYBRIDFLEX. The authors acknowledge the EPSRC (Engineering and Physical Sciences Research Council) under Grant Nos. EP/P02534X/2, EP/R511547/1, and EP/T005106/1. This work was supported by the Royal Academy of Engineering (Chair in Emerging Technologies). A.A.E., B.R., and S.S.K. acknowledge the financial support from the European Research Council under the Horizon 2020 framework program (Grant No. 772370-PHOENEX).

#### AUTHOR DECLARATIONS

##### Conflict of Interest

The authors have no conflicts to disclose.

##### Author Contributions

**Kenneth G. Latham:** Conceptualization (equal); Data curation (equal); Formal analysis (equal); Writing – original draft (equal); Writing – review & editing (equal). **Anjali Achazhiyath Edathil:** Conceptualization (equal); Writing – original draft (equal). **Babak Rezaei:** Data curation (equal); Formal analysis (equal); Writing – original draft (equal). **Sihui Liu:** Conceptualization (equal); Data

curation (equal); Writing – original draft (equal). **Sang Nguyen:** Conceptualization (equal); Data curation (equal); Writing – review & editing (equal). **Stephan Sylvest Keller:** Conceptualization (equal); Writing – original draft (equal); Writing – review & editing (equal). **Felice Torrisi:** Conceptualization (equal); Writing – original draft (equal); Writing – review & editing (equal). **Emile S. Greenhalgh:** Conceptualization (equal); Writing – original draft (equal); Writing – review & editing (equal). **Maria-Magdalena Titirici:** Conceptualization (equal); Writing – review & editing (equal).

## DATA AVAILABILITY

The data that support the findings of this study are available from the corresponding author upon reasonable request.

## REFERENCES

- A. G. Pandolfo and A. F. Hollenkamp, *J. Power Sources* **157**(1), 11–27 (2006).
- R. Nigam, K. D. Verma, T. Pal, and K. K. Kar, in *Handbook of Nanocomposite Supercapacitor Materials II: Performance*, edited by K. K. Kar (Springer International Publishing, Cham, 2020), pp. 463–481.
- M. F. Elmorshedy, M. R. Elkadeem, K. M. Kotb, I. B. M. Taha, and D. Mazzeo, *Energy Convers. Manage.* **245**, 114584 (2021).
- L. Kouchachvili, W. Yaïci, and E. Entchev, *J. Power Sources* **374**, 237–248 (2018).
- S. J. Varma, K. Sambath Kumar, S. Seal, S. Rajaraman, and J. Thomas, *Adv. Sci.* **5**(9), 1800340 (2018).
- H. Xu and M. Shen, *Int. J. Energy Res.* **45**(15), 20524–20544 (2021).
- C. Schütter, S. Pohlmann, and A. Balducci, *Adv. Energy Mater.* **9**(25), 1900334 (2019).
- Y. Jiang and J. Liu, *Energy Environ. Mater.* **2**(1), 30–37 (2019).
- D. P. Chatterjee and A. K. Nandi, *J. Mater. Chem. A* **9**(29), 15880–15918 (2021).
- Poonam, K. Sharma, A. Arora, and S. K. Tripathi, *J. Energy Storage* **21**, 801–825 (2019).
- R. Liu, A. Zhou, X. Zhang, J. Mu, H. Che, Y. Wang, T.-T. Wang, Z. Zhang, and Z. Kou, *Chem. Eng. J.* **412**, 128611 (2021).
- S. Rawat, R. K. Mishra, and T. Bhaskar, *Chemosphere* **286**(Pt. 3), 131961 (2022).
- M. J. Bleda-Martínez, J. A. Maciá-Agulló, D. Lozano-Castelló, E. Morallón, D. Cazorla-Amorós, and A. Linares-Solano, *Carbon* **43**(13), 2677–2684 (2005).
- B. Joshi, E. Samuel, Y.-i. Kim, A. L. Yarin, M. T. Swihart, and S. S. Yoon, *Coord. Chem. Rev.* **460**, 214466 (2022).
- D. Bresser, D. Buchholz, A. Moretti, A. Varzi, and S. Passerini, *Energy Environ. Sci.* **11**(11), 3096–3127 (2018).
- M. Singh, A. Gupta, S. Sundriyal, K. Jain, and S. R. Dhakate, *Mater. Chem. Phys.* **264**, 124454 (2021).
- Y. Kim, E. Samuel, B. Joshi, C. Park, H.-S. Lee, and S. S. Yoon, *Chem. Eng. J.* **420**, 130497 (2021).
- W. Qu, J. Yang, X. Sun, X. Bai, H. Jin, and M. Zhang, *Int. J. Biol. Macromol.* **189**, 768–784 (2021).
- S. A. Hosseini Ravandi, M. Sadrjehani, A. Valipouri, F. Dabirian, and F. K. Ko, *Text. Res. J.* **92**(23–24), 1–16 (2022).
- J. Chen, Z. Yu, C. Li, Y. Lv, S. Hong, P. Hu, and Y. Liu, *Macromol. Mater. Eng.* **307**, 2200057 (2022).
- A. Barhoum, K. Pal, H. Rahier, H. Uludag, I. S. Kim, and M. Bechelany, *Appl. Mater. Today* **17**, 1–35 (2019).
- S. I. Yun, S. H. Kim, D. W. Kim, Y. A. Kim, and B.-H. Kim, *Carbon* **149**, 637–645 (2019).
- A. Gopalakrishnan, P. Sahatiya, and S. Badhulika, *ChemElectroChem* **5**(3), 531–539 (2018).
- Y. Xiao, Y. Xu, K. Zhang, X. Tang, J. Huang, K. Yuan, and Y. Chen, *Carbon* **160**, 80–87 (2020).
- T. He, Q. Su, Z. Yildiz, K. Cai, and Y. Wang, *Electrochim. Acta* **222**, 1120–1127 (2016).
- P. Schlee, O. Hosseinaei, D. Baker, A. Landmér, P. Tomani, M. J. Mostazo-López, D. Cazorla-Amorós, S. Herou, and M.-M. Titirici, *Carbon* **145**, 470–480 (2019).
- P. Schlee, S. Herou, R. Jervis, P. R. Shearing, D. J. L. Brett, D. Baker, O. Hosseinaei, P. Tomani, M. M. Murshed, Y. Li, M. J. Mostazo-López, D. Cazorla-Amorós, A. B. Jorge Sobrido, and M.-M. Titirici, *Chem. Sci.* **10**(10), 2980–2988 (2019).
- G. Wang, L. Zhang, and J. Zhang, *Chem. Soc. Rev.* **41**(2), 797–828 (2012).
- N. K. Han, Y. C. Choi, D. U. Park, J. H. Ryu, and Y. G. Jeong, *Compos. Sci. Technol.* **196**, 108212 (2020).
- F. Raza, X. Ni, J. Wang, S. Liu, Z. Jiang, C. Liu, H. Chen, A. Farooq, and A. Ju, *J. Energy Storage* **30**, 101467 (2020).
- D. Wang, K. Tang, J. Xiao, X. Li, M. Long, J. Chen, H. Gao, W. Chen, C. Liu, and H. Liu, *Sustainable Mater. Technol.* **29**, e00302 (2021).
- M. Cao, W. Cheng, X. Ni, Y. Hu, and G. Han, *Electrochim. Acta* **345**, 136172 (2020).
- M. B. Poudel and H. J. Kim, *Chem. Eng. J.* **429**, 132345 (2022).
- J. Ramachandran, M. Lu, P. J. Arias-Monje, M. H. Kirmani, N. Shirolkar, and S. Kumar, *Carbon* **173**, 724–735 (2021).
- D. Han and A. J. Steckl, *ChemPlusChem* **84**(10), 1453–1497 (2019).
- J. Zhu, Q. Zhang, L. Guo, Y. Zhao, R. Zhang, L. Liu, and J. Yu, *Chem. Eng. J.* **434**, 134662 (2022).
- A. Amiri, K. Bashandeh, M. Naraghi, and A. A. Polycarpou, *Chem. Eng. J.* **409**, 128124 (2021).
- K. Asare, M. F. Hasan, A. Shahbazi, and L. Zhang, *Surf. Interfaces* **26**, 101386 (2021).
- H. Chen, N. Wang, J. Di, Y. Zhao, Y. Song, and L. Jiang, *Langmuir* **26**(13), 11291–11296 (2010).
- Y. Zhao, X. Cao, and L. Jiang, *J. Am. Chem. Soc.* **129**(4), 764–765 (2007).
- J. Li, Y. Liu, D. Zhan, Y. Zou, F. Xu, L. Sun, C. Xiang, and J. Zhang, *J. Energy Storage* **39**, 102665 (2021).
- M. Zhu, H. Liu, Q. Cao, H. Zheng, D. Xu, H. Guo, S. Wang, Y. Li, and J. Zhou, *ACS Sustainable Chem. Eng.* **8**(34), 12831–12841 (2020).
- J. Yang, Y. Wang, J. Luo, and L. Chen, *ACS Omega* **3**(4), 4647–4656 (2018).
- J. Xiong, Y. Liu, A. Li, L. Wei, L. Wang, X. Qin, and J. Yu, *Mater. Des.* **197**, 109247 (2021).
- M. Yu, R.-H. Dong, X. Yan, G.-F. Yu, M.-H. You, X. Ning, and Y.-Z. Long, *Macromol. Mater. Eng.* **302**(7), 1700002 (2017).
- L. Vyslouzilová, M. Buzgo, P. Pokorný, J. Chvojka, A. Míčková, M. Rampichová, J. Kula, K. Pejchar, M. Bílek, D. Lukáš, and E. Amler, *Int. J. Pharm.* **516**(1–2), 293–300 (2017).
- Y. Zheng, D. Ni, N. Li, W. Chen, and W. Lu, *Microporous Mesoporous Mater.* **316**, 110972 (2021).
- P. Khammantha, C. Homla-or, K. Suttisintong, J. Manyam, M. Raita, V. Champreda, V. Intasanta, H.-J. Butt, R. Berger, and A. Pangon, *ACS Appl. Nano Mater.* **4**(12), 13099–13111 (2021).
- C. Ma, L. Wu, M. Dirican, H. Cheng, J. Li, Y. Song, J. Shi, and X. Zhang, *J. Colloid Interface Sci.* **586**, 412–422 (2021).
- Y. I. Kim, E. Samuel, B. Joshi, M.-W. Kim, T. G. Kim, M. T. Swihart, and S. S. Yoon, *Chem. Eng. J.* **353**, 189–196 (2018).
- F. Miao, C. Shao, X. Li, N. Lu, K. Wang, X. Zhang, and Y. Liu, *Electrochim. Acta* **176**, 293–300 (2015).
- E. Samuel, B. Joshi, M.-W. Kim, Y.-I. Kim, M. T. Swihart, and S. S. Yoon, *Chem. Eng. J.* **371**, 657–665 (2019).
- S. Herou, J. J. Bailey, M. Kok, P. Schlee, R. Jervis, D. J. L. Brett, P. R. Shearing, M. C. Ribadeneyra, and M. Titirici, *Adv. Sci.* **8**(17), 202100016 (2021).
- E. Samuel, B. Joshi, H. S. Jo, Y. I. Kim, S. An, M. T. Swihart, J. M. Yun, K. H. Kim, and S. S. Yoon, *Chem. Eng. J.* **328**, 776–784 (2017).
- C. Zhu, T. Liu, F. Qian, W. Chen, S. Chandrasekaran, B. Yao, Y. Song, E. B. Duoss, J. D. Kuntz, C. M. Spadaccini, M. A. Worsley, and Y. Li, *Nano Today* **15**, 107–120 (2017).
- X. Tian, J. Jin, S. Yuan, C. K. Chua, S. B. Tor, and K. Zhou, *Adv. Energy Mater.* **7**(17), 1700127 (2017).

- <sup>57</sup>P. Chang, H. Mei, S. Zhou, K. G. Dassios, and L. Cheng, *J. Mater. Chem. A* **7**(9), 4230–4258 (2019).
- <sup>58</sup>H. Sun, J. Zhu, D. Baumann, L. Peng, Y. Xu, I. Shakir, Y. Huang, and X. Duan, *Nat. Rev. Mater.* **4**(1), 45–60 (2018).
- <sup>59</sup>K. Fu, Y. Yao, J. Dai, and L. Hu, *Adv. Mater.* **29**(9), 1603486 (2017).
- <sup>60</sup>M. Cheng, R. Deivanayagam, and R. Shahbazian-Yassar, *Batteries Supercaps* **3**(2), 130–146 (2020).
- <sup>61</sup>F. Zhang, M. Wei, V. V. Viswanathan, B. Swart, Y. Shao, G. Wu, and C. Zhou, *Nano Energy* **40**, 418–431 (2017).
- <sup>62</sup>D. Gu, *Laser Additive Manufacturing of High-Performance Materials* (Springer, 2015).
- <sup>63</sup>A. Tanwilaisiri and P. Kajondecha, in *2021 9th International Electrical Engineering Congress (IIECON)* (IEEE, 2021), pp. 117–120.
- <sup>64</sup>F. Torrisi and T. Carey, *Nano Today* **23**, 73–96 (2018).
- <sup>65</sup>W. Yang, J. Yang, J. J. Byun, F. P. Moissinac, J. Xu, S. J. Haigh, M. Domingos, M. A. Bissett, R. A. W. Dryfe, and S. Barg, *Adv. Mater.* **31**(37), 1902725 (2019).
- <sup>66</sup>B. Yao, S. Chandrasekaran, J. Zhang, W. Xiao, F. Qian, C. Zhu, E. B. Duoss, C. M. Spadaccini, M. A. Worsley, and Y. Li, *Joule* **3**(2), 459–470 (2019).
- <sup>67</sup>X. Tian, *2D Mater.* **9**(1), 012001 (2021).
- <sup>68</sup>S. Wünscher, R. Abbel, J. Perelaer, and U. S. Schubert, *J. Mater. Chem. C* **2**(48), 10232–10261 (2014).
- <sup>69</sup>Q. Ge, Z. Li, Z. Wang, K. Kowsari, W. Zhang, X. He, J. Zhou, and N. X. Fang, *Int. J. Extreme Manuf.* **2**(2), 022004 (2020).
- <sup>70</sup>C. Sun, N. Fang, D. M. Wu, and X. Zhang, *Sens. Actuators, A* **121**(1), 113–120 (2005).
- <sup>71</sup>B. Rezaei, J. Y. Pan, C. Gundlach, and S. S. Keller, *Mater. Des.* **193**, 108834 (2020).
- <sup>72</sup>B. Rezaei, T. W. Hansen, and S. S. Keller, *ACS Appl. Nano Mater.* **5**(2), 1808–1819 (2022).
- <sup>73</sup>R.-w. Fu, Z.-h. Li, Y.-r. Liang, F. Li, F. Xu, and D.-c. Wu, *New Carbon Mater.* **26**(3), 171–179 (2011).
- <sup>74</sup>J. Yin, W. Zhang, N. A. Alhebshi, N. Salah, and H. N. Alshareef, *Small Methods* **4**(3), 1900853 (2020).
- <sup>75</sup>W. He, R. Ma, and D. J. Kang, *Carbon* **161**, 117–122 (2020).
- <sup>76</sup>C. Zhao, C. Wang, R. Gorkin, S. Beirne, K. Shu, and G. G. Wallace, *Electrochem. Commun.* **41**, 20–23 (2014).
- <sup>77</sup>D. Zhang, B. Chi, B. Li, Z. Gao, Y. Du, J. Guo, and J. Wei, *Synth. Met.* **217**, 79–86 (2016).
- <sup>78</sup>M. Areir, Y. Xu, R. Zhang, D. Harrison, J. Fyson, and E. Pei, *J. Manuf. Process.* **25**, 351–356 (2017).
- <sup>79</sup>Y. Wang, M. Mehrali, Y.-Z. Zhang, M. A. Timmerman, B. A. Boukamp, P.-Y. Xu, and J. E. ten Elshof, *Energy Storage Mater.* **36**, 318–325 (2021).
- <sup>80</sup>W. Liu, C. Lu, H. Li, R. Y. Tay, L. Sun, X. Wang, W. L. Chow, X. Wang, B. K. Tay, Z. Chen, J. Yan, K. Feng, G. Lui, R. Tjandra, L. Rasenthiram, G. Chiu, and A. Yu, *J. Mater. Chem. A* **4**(10), 3754–3764 (2016).
- <sup>81</sup>K.-H. Choi, J. Yoo, C. K. Lee, and S.-Y. Lee, *Energy Environ. Sci.* **9**(9), 2812–2821 (2016).
- <sup>82</sup>Y. Liu, B. Zhang, Q. Xu, Y. Hou, S. Seyedin, S. Qin, G. G. Wallace, S. Beirne, J. M. Razal, and J. Chen, *Adv. Funct. Mater.* **28**(21), 1706592 (2018).
- <sup>83</sup>J. Bauer, A. Schroer, R. Schwaiger, and O. Kraft, *Nat. Mater.* **15**(4), 438–443 (2016).
- <sup>84</sup>R. M. Hensleigh, H. Cui, J. S. Oakdale, J. C. Ye, P. G. Campbell, E. B. Duoss, C. M. Spadaccini, X. Zheng, and M. A. Worsley, *Mater. Horiz.* **5**(6), 1035–1041 (2018).
- <sup>85</sup>J. Xue, L. Gao, X. Hu, K. Cao, W. Zhou, W. Wang, and Y. Lu, *Nano-Micro Lett.* **11**(1), 46 (2019).
- <sup>86</sup>S. H. Park, M. Kaur, D. Yun, and W. S. Kim, *Langmuir* **34**(37), 10897–10904 (2018).
- <sup>87</sup>K. Narita, M. A. Citrin, H. Yang, X. Xia, and J. R. Greer, *Adv. Energy Mater.* **11**(5), 2002637 (2020).
- <sup>88</sup>P. Wang, H. Zhang, H. Wang, D. Li, J. Xuan, and L. Zhang, *Adv. Mater. Technol.* **5**(6), 1901030 (2020).
- <sup>89</sup>J. Y. Pan, B. Rezaei, T. A. Anhöj, N. B. Larsen, and S. S. Keller, *Micro Nano Eng.* **15**, 100124 (2022).
- <sup>90</sup>M. Beidaghi and C. Wang, *Proc. SPIE* **8377**, 837708–837710 (2012).
- <sup>91</sup>M. M. Amaral, R. Venâncio, A. C. Peterlevitz, and H. Zanin, *J. Energy Chem.* **67**, 697–717 (2022).
- <sup>92</sup>J. Zhong, L.-Q. Fan, X. Wu, J.-H. Wu, G.-J. Liu, J.-M. Lin, M.-L. Huang, and Y.-L. Wei, *Electrochim. Acta* **166**, 150–156 (2015).
- <sup>93</sup>A. Jain and S. K. Tripathi, *J. Solid State Electrochem.* **17**(9), 2545–2550 (2013).
- <sup>94</sup>K. Sun, E. Feng, H. Peng, G. Ma, Y. Wu, H. Wang, and Z. Lei, *Electrochim. Acta* **158**, 361–367 (2015).
- <sup>95</sup>M. Xia, J. Nie, Z. Zhang, X. Lu, and Z. L. Wang, *Nano Energy* **47**, 43–50 (2018).
- <sup>96</sup>S. Qin, S. Seyedin, J. Zhang, Z. Wang, F. Yang, Y. Liu, J. Chen, and J. M. Razal, *Macromol. Rapid Commun.* **39**(13), 1800103 (2018).
- <sup>97</sup>Y. Fu, H. Wu, S. Ye, X. Cai, X. Yu, S. Hou, H. Kafafy, and D. Zou, *Energy Environ. Sci.* **6**(3), 805 (2013).
- <sup>98</sup>Z. Lu, Y. Chao, Y. Ge, J. Foroughi, Y. Zhao, C. Wang, H. Long, and G. G. Wallace, *Nanoscale* **9**(16), 5063–5071 (2017).
- <sup>99</sup>T. Chen, L. Qiu, Z. Yang, Z. Cai, J. Ren, H. Li, H. Lin, X. Sun, and H. Peng, *Angew. Chem., Int. Ed. Engl.* **51**(48), 11977–11980 (2012).
- <sup>100</sup>H. Sun, X. You, J. Deng, X. Chen, Z. Yang, P. Chen, X. Fang, and H. Peng, *Angew. Chem., Int. Ed. Engl.* **53**(26), 6664–6668 (2014).
- <sup>101</sup>P. Simon and Y. Gogotsi, *Nat. Mater.* **19**(11), 1151–1163 (2020).
- <sup>102</sup>S. Lage-Rivera, A. Ares-Pernas, and M. J. Abad, *Int. J. Energy Res.* **46**(8), 10475–10498 (2022).
- <sup>103</sup>Y. Meng, Y. Zhao, C. Hu, H. Cheng, Y. Hu, Z. Zhang, G. Shi, and L. Qu, *Adv. Mater.* **25**(16), 2326–2331 (2013).
- <sup>104</sup>G. Eda, G. Fanchini, and M. Chhowalla, *Nat. Nanotechnol.* **3**(5), 270–274 (2008).
- <sup>105</sup>Z. Ling, C. E. Ren, M.-Q. Zhao, J. Yang, J. M. Giammarco, J. Qiu, M. W. Barsoum, and Y. Gogotsi, *Proc. Natl. Acad. Sci. U. S. A.* **111**(47), 16676–16681 (2014).
- <sup>106</sup>S. Qiang, T. Carey, A. Arbab, W. Song, C. Wang, and F. Torrisi, *Nanoscale* **11**(20), 9912–9919 (2019).
- <sup>107</sup>M. Acerce, D. Voiry, and M. Chhowalla, *Nat. Nanotechnol.* **10**(4), 313–318 (2015).
- <sup>108</sup>S. Seyedin, T. Carey, A. Arbab, L. Eskandarian, S. Bohm, J. M. Kim, and F. Torrisi, *Nanoscale* **13**(30), 12818–12847 (2021).
- <sup>109</sup>D. Yu, Q. Qian, L. Wei, W. Jiang, K. Goh, J. Wei, J. Zhang, and Y. Chen, *Chem. Soc. Rev.* **44**(3), 647–662 (2015).
- <sup>110</sup>A. Yu, I. Roes, A. Davies, and Z. Chen, *Appl. Phys. Lett.* **96**(25), 253105 (2010).
- <sup>111</sup>G. Qu, J. Cheng, X. Li, D. Yuan, P. Chen, X. Chen, B. Wang, and H. Peng, *Adv. Mater.* **28**(19), 3646–3652 (2016).
- <sup>112</sup>X. Cai, M. Peng, X. Yu, Y. Fu, and D. Zou, *J. Mater. Chem. C* **2**(7), 1184–1200 (2014).
- <sup>113</sup>V. T. Le, H. Kim, A. Ghosh, J. Kim, J. Chang, Q. A. Vu, D. T. Pham, J.-H. Lee, S.-W. Kim, and Y. H. Lee, *ACS Nano* **7**(7), 5940–5947 (2013).
- <sup>114</sup>Y. Shang, X. He, Y. Li, L. Zhang, Z. Li, C. Ji, E. Shi, P. Li, K. Zhu, Q. Peng, C. Wang, X. Zhang, R. Wang, J. Wei, K. Wang, H. Zhu, D. Wu, and A. Cao, *Adv. Mater.* **24**(21), 2896–2900 (2012).
- <sup>115</sup>J. Ren, L. Li, C. Chen, X. Chen, Z. Cai, L. Qiu, Y. Wang, X. Zhu, and H. Peng, *Adv. Mater.* **25**(8), 1155–1159, 1224 (2013).
- <sup>116</sup>Y. Zhang, W. Bai, X. Cheng, J. Ren, W. Weng, P. Chen, X. Fang, Z. Zhang, and H. Peng, *Angew. Chem., Int. Ed. Engl.* **53**(52), 14564–14568 (2014).
- <sup>117</sup>X. Xiao, T. Li, P. Yang, Y. Gao, H. Jin, W. Ni, W. Zhan, X. Zhang, Y. Cao, J. Zhong, L. Gong, W.-C. Yen, W. Mai, J. Chen, K. Huo, Y.-L. Chueh, Z. L. Wang, and J. Zhou, *ACS Nano* **6**(10), 9200–9206 (2012).
- <sup>118</sup>J. Bae, Y. J. Park, M. Lee, S. N. Cha, Y. J. Choi, C. S. Lee, J. M. Kim, and Z. L. Wang, *Adv. Mater.* **23**(30), 3446–3449 (2011).
- <sup>119</sup>D. Yu, K. Goh, H. Wang, L. Wei, W. Jiang, Q. Zhang, L. Dai, and Y. Chen, *Nat. Nanotechnol.* **9**(7), 555–562 (2014).
- <sup>120</sup>X. Wang, B. Liu, R. Liu, Q. Wang, X. Hou, D. Chen, R. Wang, and G. Shen, *Angew. Chem., Int. Ed. Engl.* **53**(7), 1849–1853 (2014).
- <sup>121</sup>Z. Pan, J. Yang, L. Li, X. Gao, L. Kang, Y. Zhang, Q. Zhang, Z. Kou, T. Zhang, L. Wei, Y. Yao, and J. Wang, *Energy Storage Mater.* **25**, 124–130 (2020).
- <sup>122</sup>A. Lund, Y. Wu, B. Fenech-Salerno, F. Torrisi, T. B. Carmichael, and C. Müller, *MRS Bull.* **46**(6), 491–501 (2021).

- <sup>123</sup>W. Liu, M.-S. Song, B. Kong, and Y. Cui, *Adv. Mater.* **29**(1), 1603436 (2017).
- <sup>124</sup>A. Whitmore, A. Agarwal, and L. Da Xu, *Inf. Syst. Front.* **17**(2), 261–274 (2014).
- <sup>125</sup>Y. Xu, W. Lu, G. Xu, and T.-W. Chou, *Compos. Sci. Technol.* **204**, 108636 (2021).
- <sup>126</sup>C. González, J. J. Vilatela, J. M. Molina-Aldareguía, C. S. Lopes, and J. Llorca, *Prog. Mater. Sci.* **89**, 194–251 (2017).
- <sup>127</sup>H. Zhou, H. Li, L. Li, T. Liu, G. Chen, Y. Zhu, L. Zhou, and H. Huang, *Mater. Today Energy* **24**, 100924 (2022).
- <sup>128</sup>K.-Y. Chan, B. Jia, H. Lin, N. Hameed, J.-H. Lee, and K.-T. Lau, *Compos. Struct.* **188**, 126–142 (2018).
- <sup>129</sup>S. N. Nguyen, A. Millereux, A. Pouyat, E. S. Greenhalgh, M. S. P. Shaffer, A. R. J. Kucernak, and P. Linde, *J. Aircr.* **58**(3), 677–687 (2021).
- <sup>130</sup>E. Karadotcheva, S. N. Nguyen, E. S. Greenhalgh, M. S. P. Shaffer, A. R. J. Kucernak, and P. Linde, *Energies* **14**(19), 6006 (2021).
- <sup>131</sup>S. Nguyen, D. B. Anthony, H. Qian, C. Yue, A. Singh, A. Bismarck, M. S. P. Shaffer, and E. S. Greenhalgh, *Compos. Sci. Technol.* **182**, 107720 (2019).
- <sup>132</sup>G. Qi, S. Nguyen, D. B. Anthony, A. R. J. Kucernak, M. S. P. Shaffer, and E. S. Greenhalgh, *Multifunct. Mater.* **4**(3), 034001 (2021).
- <sup>133</sup>H. Qian, A. R. Kucernak, E. S. Greenhalgh, A. Bismarck, and M. S. P. Shaffer, *ACS Appl. Mater. Interfaces* **5**(13), 6113–6122 (2013).
- <sup>134</sup>A. Javaid, O. Khalid, A. Shakeel, and S. Noreen, *J. Energy Storage* **33**, 102168 (2021).
- <sup>135</sup>B. K. Deka, A. Hazarika, J. Kim, Y.-B. Park, and H. W. Park, *Composites, Part A* **87**, 256–262 (2016).
- <sup>136</sup>B. K. Deka, A. Hazarika, O. Kwon, D. Kim, Y.-B. Park, and H. W. Park, *Chem. Eng. J.* **325**, 672–680 (2017).
- <sup>137</sup>B. K. Deka, A. Hazarika, J. Kim, N. Kim, H. E. Jeong, Y.-B. Park, and H. W. Park, *Chem. Eng. J.* **355**, 551–559 (2019).
- <sup>138</sup>B. K. Deka, A. Hazarika, S. Lee, D. Y. Kim, Y.-B. Park, and H. W. Park, *Nano Energy* **73**, 104754 (2020).
- <sup>139</sup>N. Shirshova, H. Qian, M. Houllé, J. H. G. Steinke, A. R. J. Kucernak, Q. P. V. Fontana, E. S. Greenhalgh, A. Bismarck, and M. S. P. Shaffer, *Faraday Discuss.* **172**, 81–103 (2014).
- <sup>140</sup>V. Tu, L. E. Asp, N. Shirshova, F. Larsson, K. Runesson, and R. Jänicke, *Multifunct. Mater.* **3**(2), 025001 (2020).
- <sup>141</sup>J. F. Snyder, R. H. Carter, and E. D. Wetzel, *Chem. Mater.* **19**(15), 3793–3801 (2007).
- <sup>142</sup>J. F. Snyder, E. D. Wetzel, and C. M. Watson, *Polymer* **50**(20), 4906–4916 (2009).
- <sup>143</sup>Q. Wendong, J. Dent, V. Arrighi, L. Cavalcanti, M. S. P. Shaffer, and N. Shirshova, *Multifunct. Mater.* **4**(3), 035003 (2021).
- <sup>144</sup>P.-A. T. Nguyen and J. Snyder, *ECS Meet. Abstr. MA2007-02*, 170 (2007).
- <sup>145</sup>L. H. Acauan, Y. Zhou, E. Kalfon-Cohen, N. K. Fritz, and B. L. Wardle, *Nanoscale* **11**(45), 21964–21973 (2019).
- <sup>146</sup>A. Kwade, W. Haselrieder, R. Leithoff, A. Modlinger, F. Dietrich, and K. Droeder, *Nat. Energy* **3**(4), 290–300 (2018).
- <sup>147</sup>M. Valkova, Ph.D. thesis, Imperial College London, 2022.
- <sup>148</sup>D. B. Anthony, S. Greenhalgh Emile, T. Katafiasz, A. R. J. Kucernak, P. Linde, S. Nguyen, G. Qi, S. Razavi, E. Senokos, M. S. P. Shaffer, and M. Valkova, in 20th European Conference on Composite Materials, Lausanne, Switzerland, 2022.
- <sup>149</sup>P. Svens, M. Kjell, C. Tengstedt, G. Flodberg, and G. Lindbergh, *Energies* **6**(1), 400–410 (2013).
- <sup>150</sup>X. Yu, Y. Wang, L. Li, H. Li, and Y. Shang, *Sci. Rep.* **7**, 45378 (2017).
- <sup>151</sup>K. Liu, C. Yu, W. Guo, L. Ni, J. Yu, Y. Xie, Z. Wang, Y. Ren, and J. Qiu, *J. Energy Chem.* **58**, 94–109 (2021).